ONLINE MODEL-BASED STRUCTURAL DAMAGE DETECTION IN ELECTRONIC ASSEMBLIES

Emmanuel A. Ogunniyi [1], Joud Satme [1], Austin R.J. Downey [1,2]
[1]Department of Mechanical Engineering, University of South Carolina, Columbia, USA
[2]Department of Civil and Environmental Engineering, University of South Carolina, Columbia, USA

UNIVERSITY OF
SOUTH CAROLINA

Contents

High-rate Dynamics in the Real-world

Civil Structures Exposed to blast

Samali, B., et al., *Review of the basics of state of the art of blast loading. Asian Journal of Civil Engineering.* (2018).

Automotive safety systems against Collision

airbag deployment

Space shuttle and Aerial Vehicles Prone to In-Flight Anomalies

Hypersonic vehicles

Ballistic packages

Debris approaching space shuttle

Lightning strikes on aircraft

Fighter jets

Description of High-rate Dynamics

High-rate (<100ms)

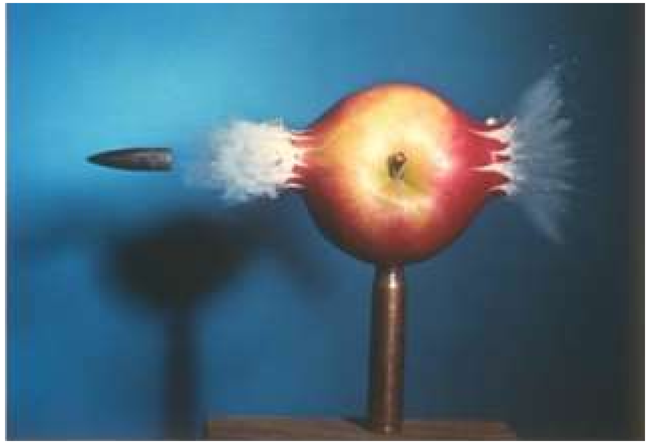

High-amplitude (acceleration > 100 g)

The deceleration event in drop tower tests typically lasts for 0.5ms

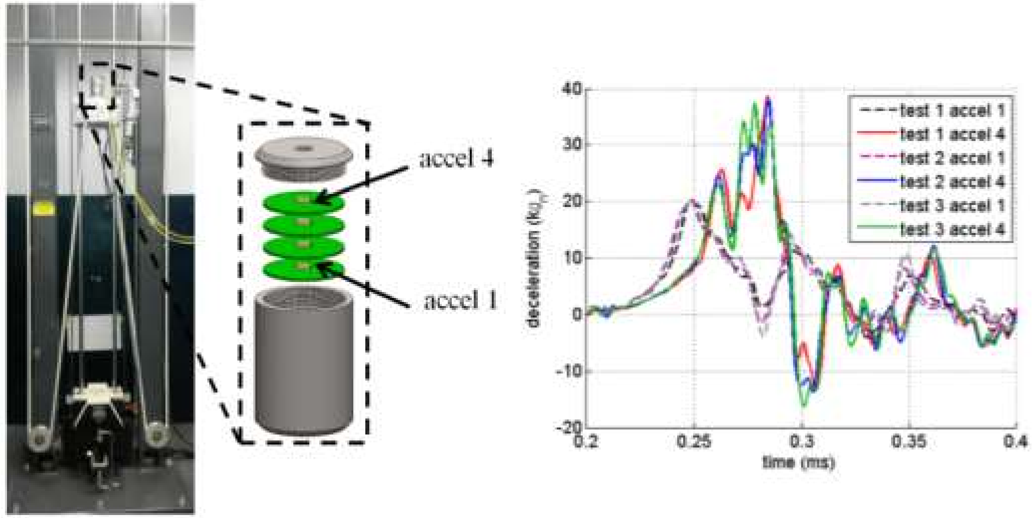

- Large uncertainties in the external loads.
- High levels of nonstationarity and heavy disturbance.
- Generations of unmodeled dynamics from changes in mechanical configuration.

GitHub

Hong, J. et al,. *Introduction to state estimation of high-rate system dynamics*. Sensors, 18(2):217, Jan 2018

Experimental System used for Validation

- The Dynamic Reproduction of Projectiles in Ballistic Environments for Advanced Research (DROPBEAR) was used to generate the experimental data in this work.

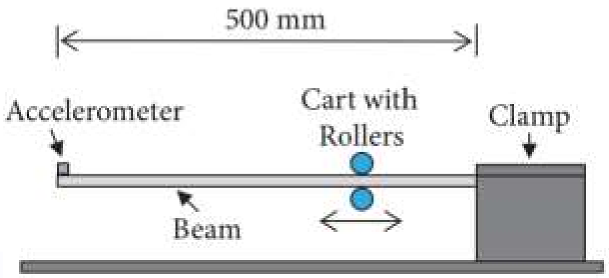

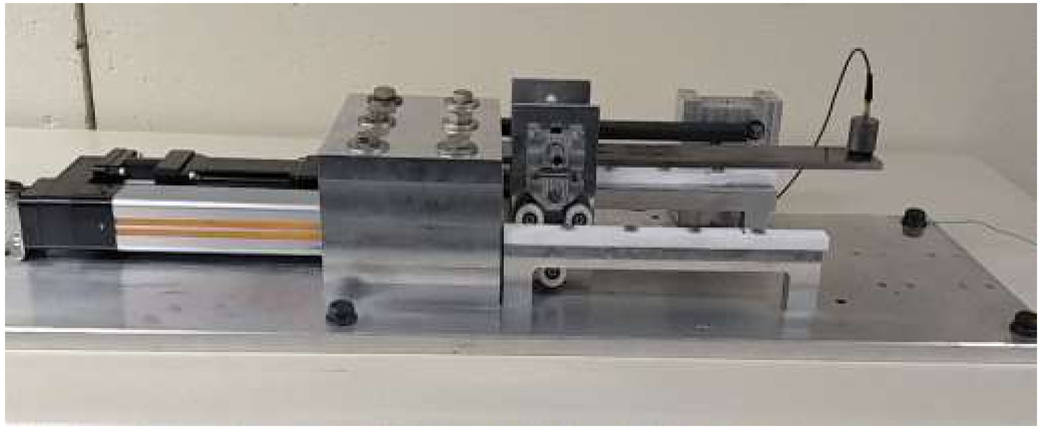

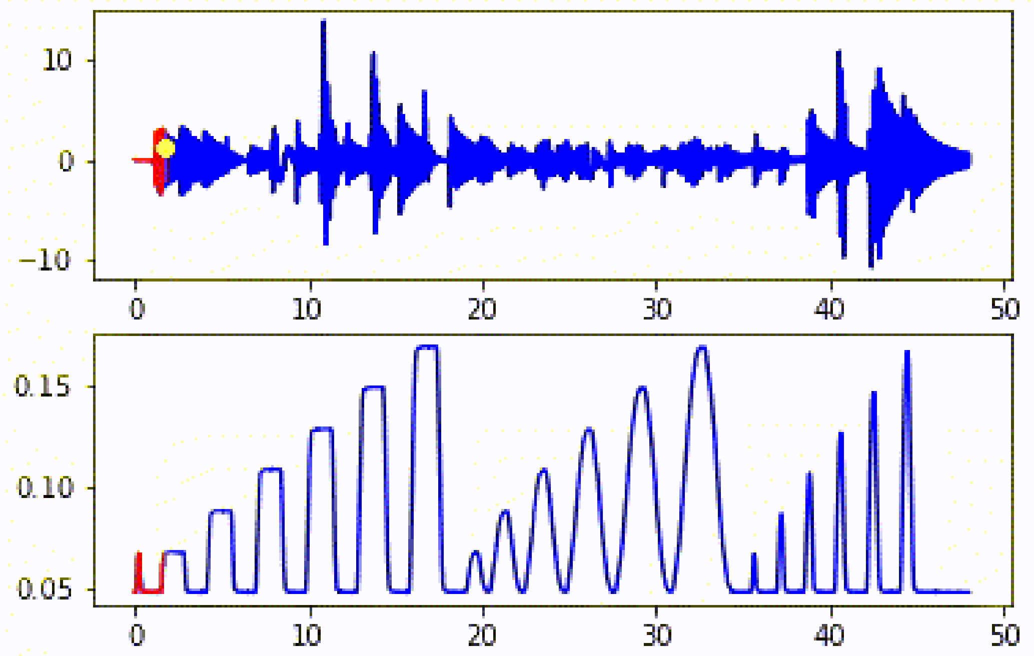

Joyce, B., Dodson, J., Laflamme, S., & Hong, J. *An experimental test bed for developing high-rate structural health monitoring methods*. Shock and Vibration, 2018.

Real-time FEA model updating (1D)

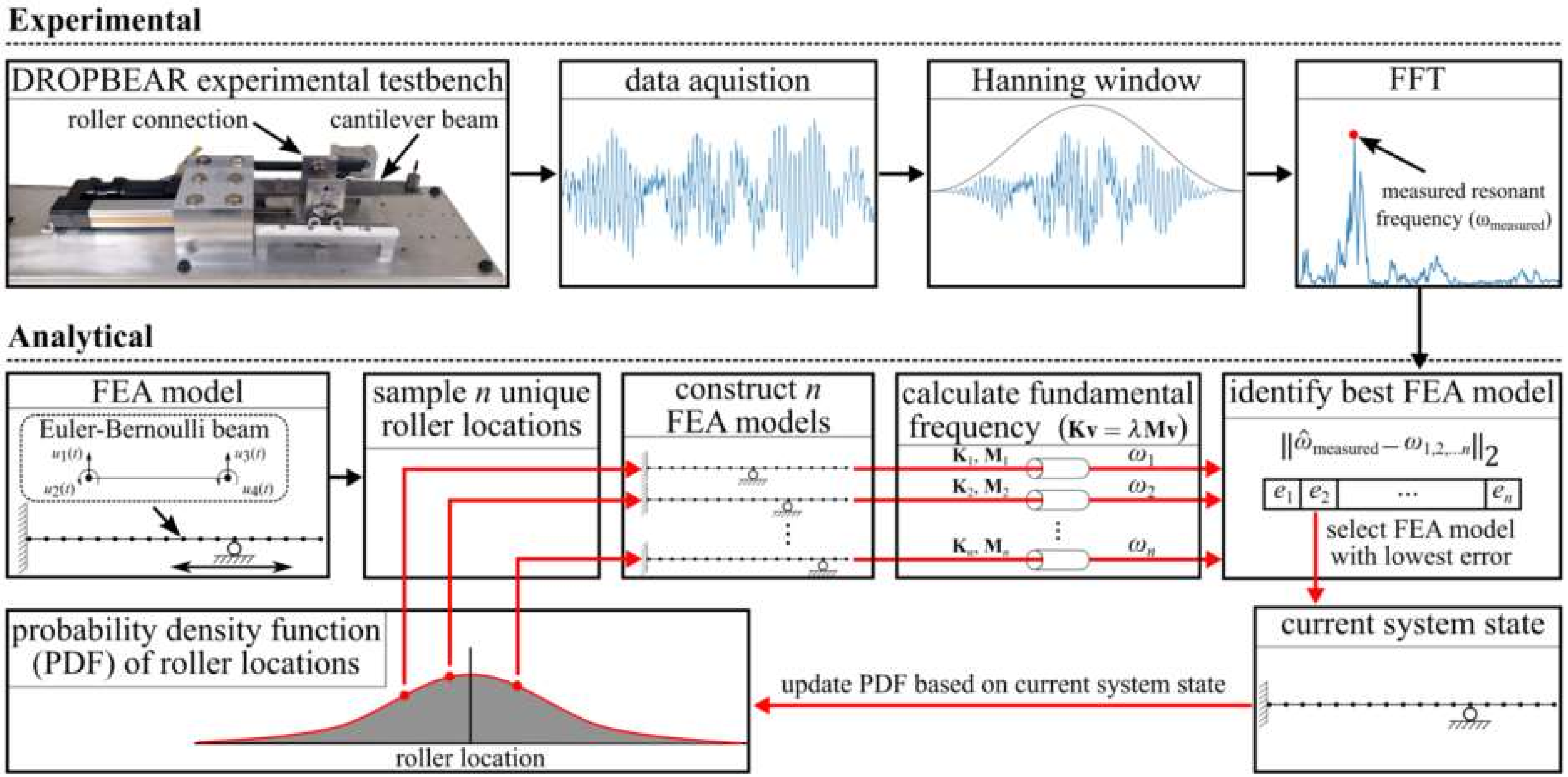

Downey A., et al,. “Millisecond Model Updating for Structures Experiencing Unmodeled High-Rate Dynamic Events” *Mechanical Systems and Signal Processing* ***138***, 2020

Real-time FEA model updating Results

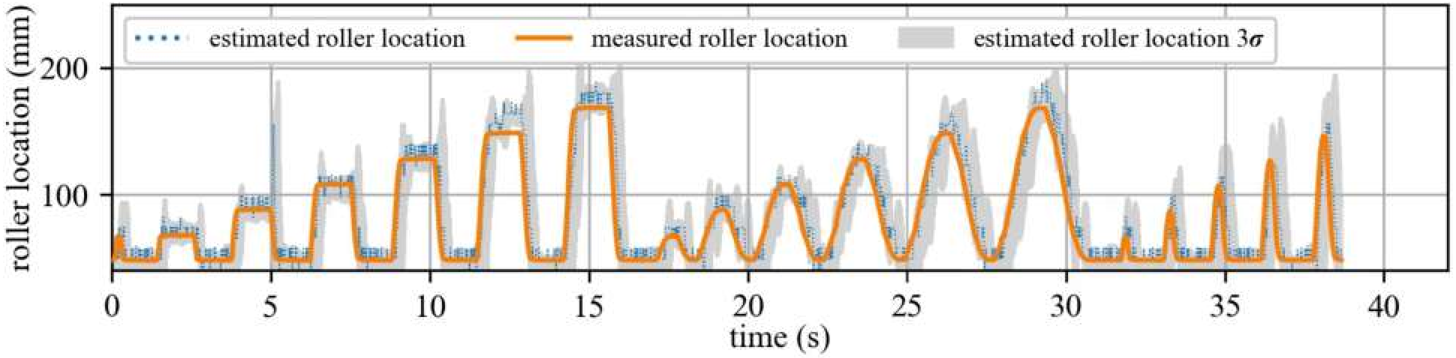

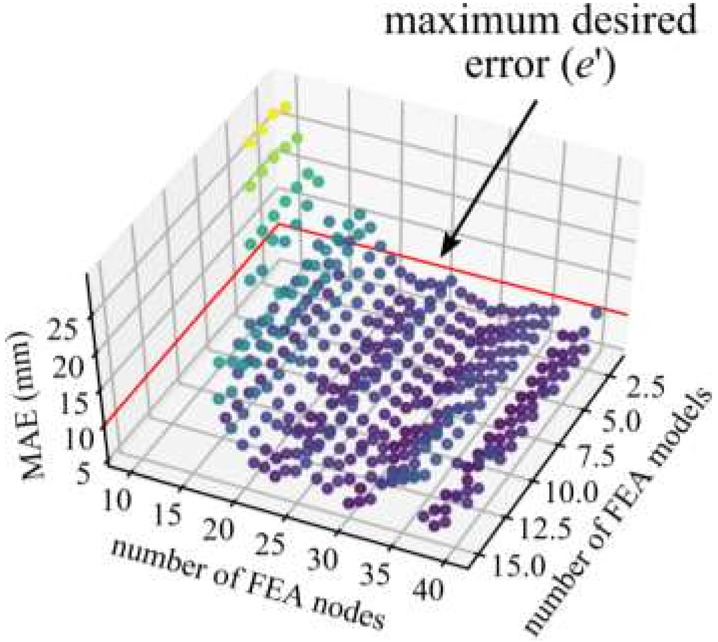

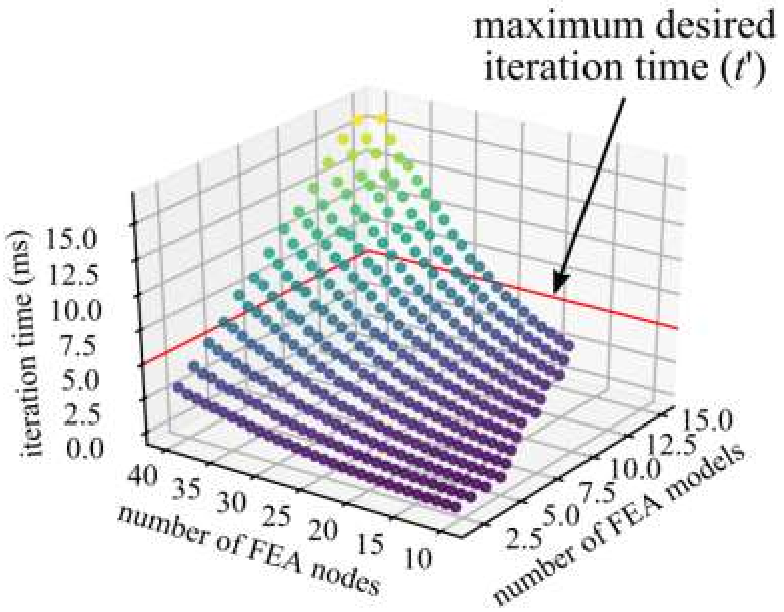

Downey A., et al,. "Millisecond Model Updating for Structures Experiencing Unmodeled High-Rate Dynamic Events" *Mechanical Systems and Signal Processing* ***138***, 2020

FEA Computation speed for the DROPBEAR

General Eigenvalue solutions accurately estimates the state of the DROPBEAR

Solving for system's frequencies accounted for 90% of algorithm iteration time

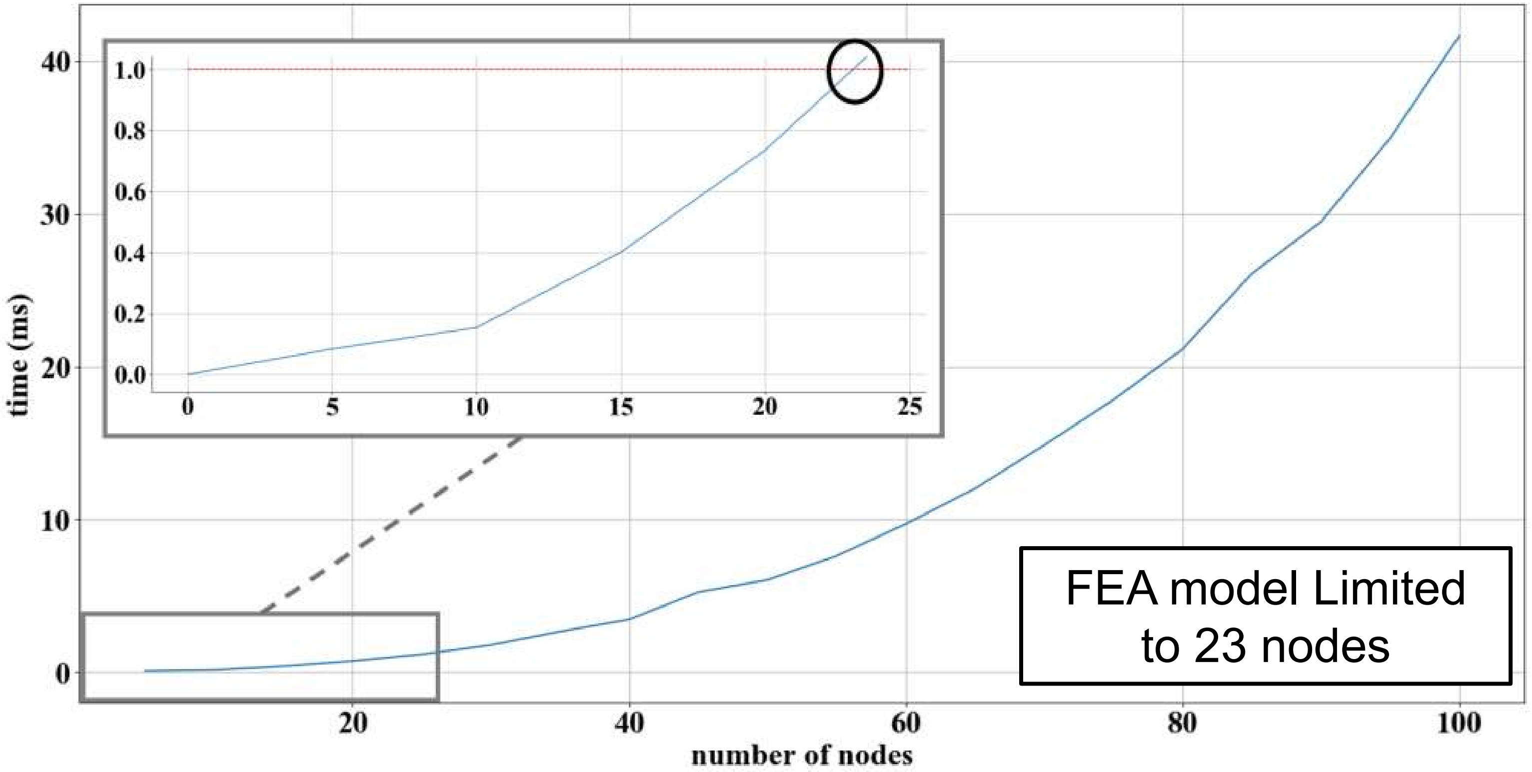

Carroll, M., Downey, A., Dodson, J., Hong, J. and Scheppegrell, J., "Analysis of Computation Speeds of Eigenvalue Solutions for High-Rate Structural Health Monitoring."

Local Eigenvalue Modification Procedure (LEMP)

- Developed by Wesseinburger in 1968
- Identifies physical changes to the system such as mass, stiffness or damping using changes such as frequencies or mode shapes
- Model the altered state as a mixture of the initial state and changes made to the initial state
- Reduces the GE equation to a set of second-order equations

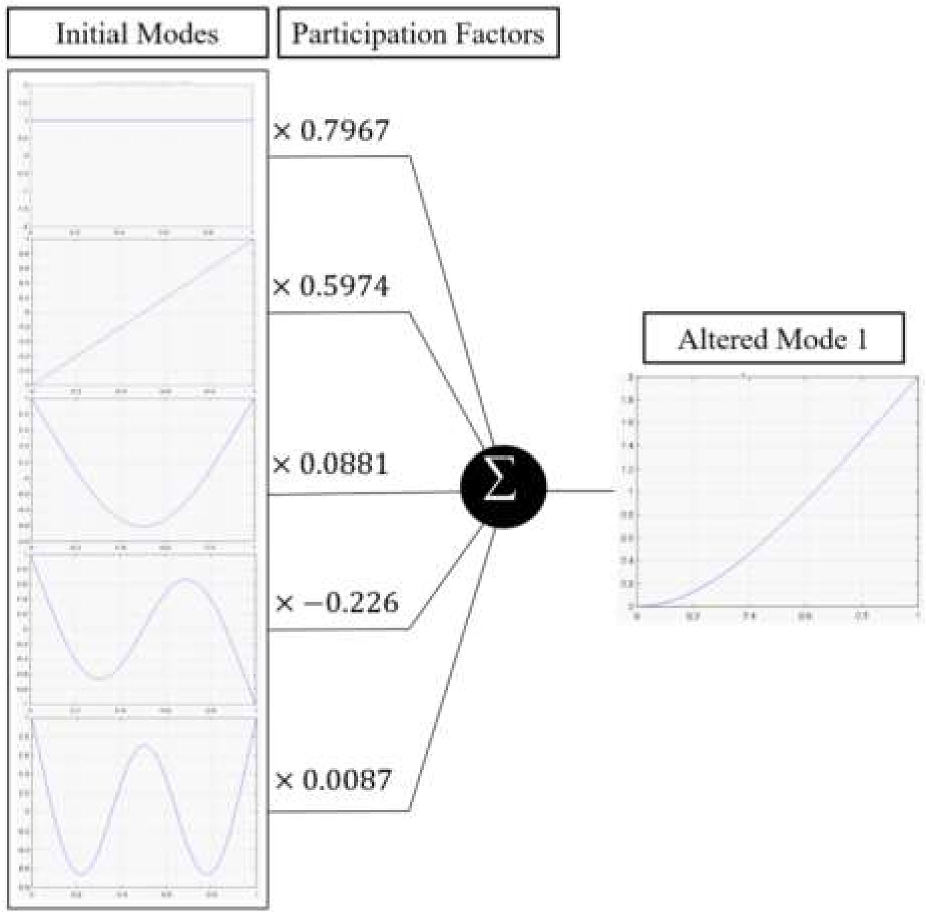

Avitabile, P., "*Twenty Years of Structural Dynamic Modification- A Review*," *Sound and Vibration*, pp. 14-25. 2003
Drnek, C. R., "*Local eigenvalue modification procedure for real-time model updating of structures experiencing high-rate dynamic events*," (2020).

1D vs 2D Structural systems

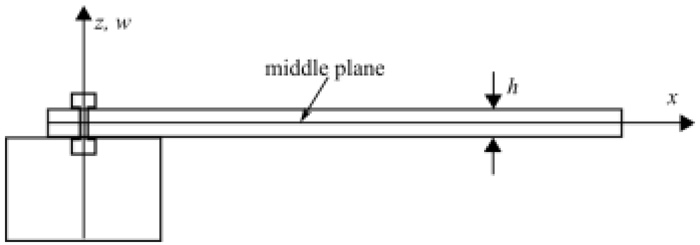

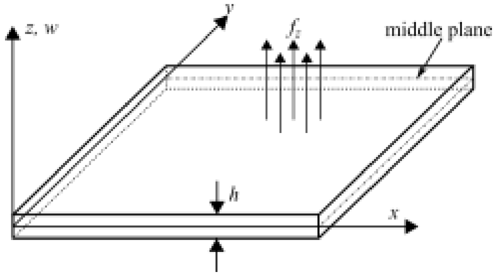

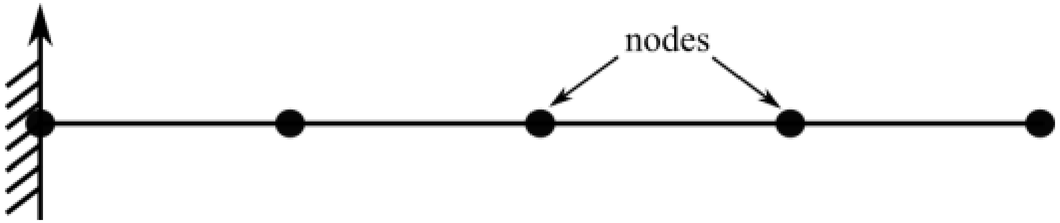

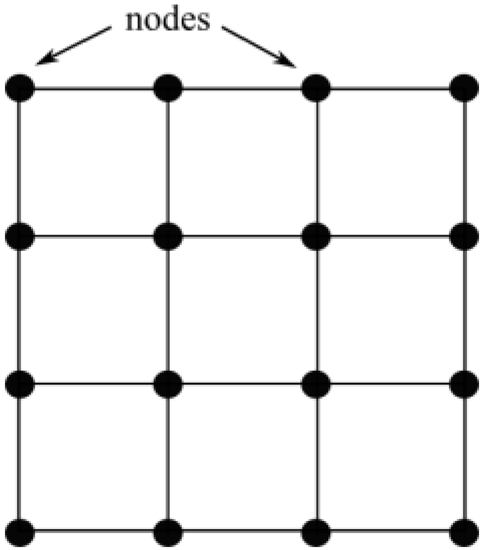

Current methodology

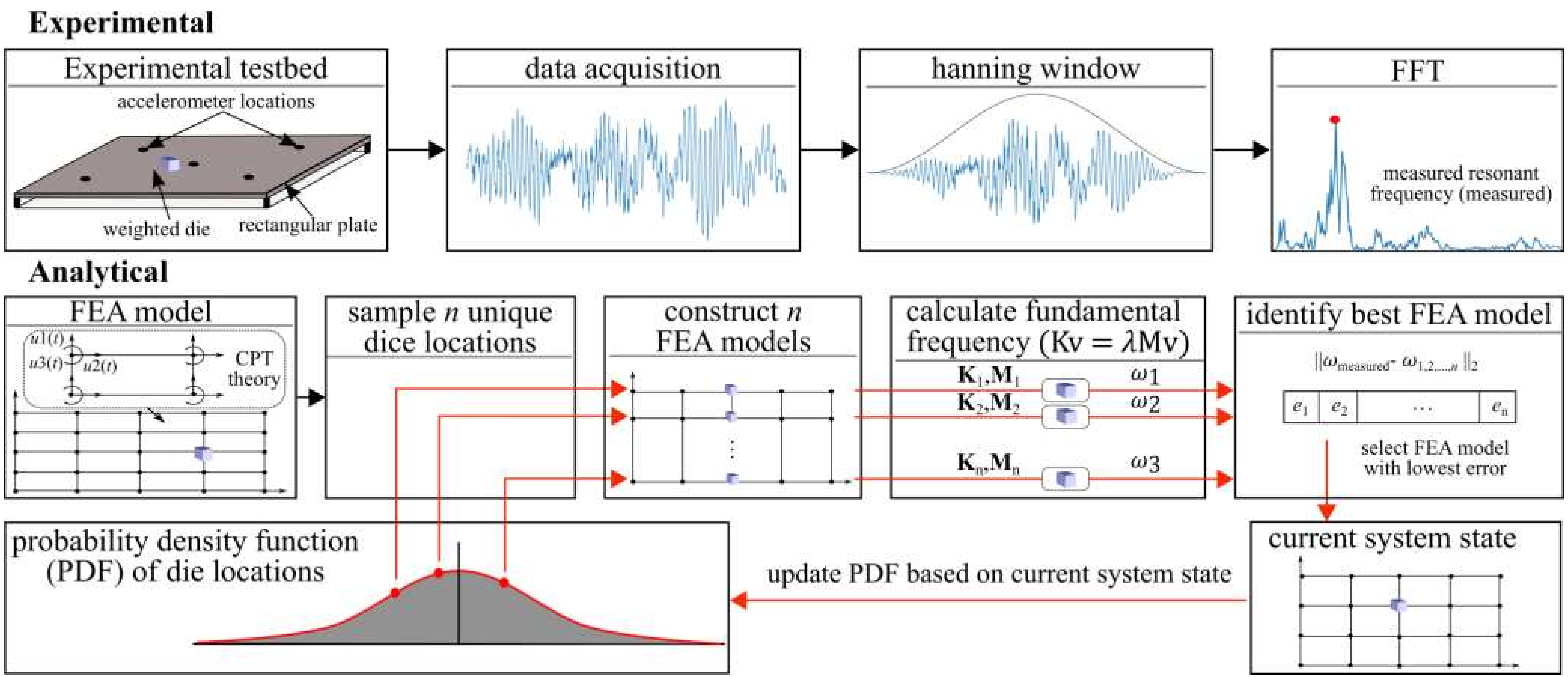

2D Model Formulation

Shell element

Mindlin plate theorem

Three translational displacements in the x, y, and z directions, and three rotational deformations with respect to the x, y, and z axes.

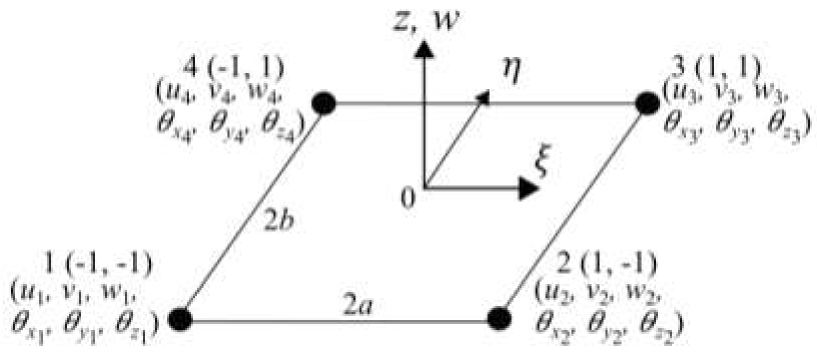

$$\mathbf{d}_e = \begin{Bmatrix} \mathbf{d}_1 \\ \mathbf{d}_2 \\ \mathbf{d}_3 \\ \mathbf{d}_4 \end{Bmatrix} \begin{matrix} \text{node 1} \\ \text{node 2} \\ \text{node 3} \\ \text{node 4} \end{matrix}$$

where $\mathbf{d}_i$ (i=1, 2, 3, 4) are the displacement vector at node i:

$$\mathbf{d}_i = \begin{Bmatrix} u_i \\ v_i \\ w_i \\ \theta_{xi} \\ \theta_{yi} \\ \theta_{zi} \end{Bmatrix} \begin{matrix} \text{displacement in } x \text{ direction} \\ \text{displacement in } y \text{ direction} \\ \text{displacement in } z \text{ direction} \\ \text{rotation about } x\text{-axis} \\ \text{rotation about } y\text{-}axis \\ \text{rotation about } z\text{-axis} \end{matrix}$$

2D Model Formulation

Calculation of k_e and m_e using shape functions N and strain matrix in step 2. to obtain Eqs. 6 and 7.

mass matrix

$$\mathbf{m}_\mathrm{e} = \int_A h\rho \mathbf{N}^\mathrm{T}\mathbf{N}\mathrm{dA}, \qquad \mathbf{m}_\mathrm{p} = \int_{A_p} \mathbf{N}^\mathrm{T}\mathbf{I}\mathbf{N}\mathrm{dA} \quad (6)$$

$$\mathbf{I} = \begin{bmatrix} \rho h & 0 & 0 \\ 0 & \rho h^3/12 & 0 \\ 0 & 0 & \rho h^3/12 \end{bmatrix}$$

stiffness matrix

$$\mathbf{k}_\mathrm{e} = \int_A h\mathbf{B}^\mathrm{T}\mathbf{c}\mathbf{B}\mathrm{dA}, \qquad \mathbf{k}_\mathrm{p} = \int_{A_p} \frac{h^3}{12}\left[\mathbf{B}^\mathrm{I}\right]^\mathrm{T}\mathbf{c}\mathbf{B}^\mathrm{I} dA + \int_{A_p} \kappa h \left[\mathbf{B}^\mathrm{O}\right]^\mathrm{T}\mathbf{c}_s\mathbf{B}^\mathrm{O} dA \quad (7)$$

2D Model Formulation

Mass matrix superposition

$$\mathbf{m} = \begin{array}{c} \begin{array}{cccc} \overbrace{\qquad\qquad\qquad}^{\text{node 1}} & \overbrace{\qquad\qquad\qquad}^{\text{node 2}} & \overbrace{\qquad\qquad\qquad}^{\text{node 3}} & \overbrace{\qquad\qquad\qquad}^{\text{node 4}} \end{array} \\ \left[\begin{array}{cccccccccccc} \mathbf{m}^m_{11} & \mathbf{0} & 0 & \mathbf{m}^m_{12} & \mathbf{0} & 0 & \mathbf{m}^m_{13} & \mathbf{0} & 0 & \mathbf{m}^m_{14} & \mathbf{0} & 0 \\ \mathbf{0} & \mathbf{m}^b_{11} & 0 & \mathbf{0} & \mathbf{m}^b_{12} & 0 & \mathbf{0} & \mathbf{m}^b_{13} & 0 & \mathbf{0} & \mathbf{m}^b_{14} & 0 \\ 0 & 0 & 0 & 0 & 0 & 0 & 0 & 0 & 0 & 0 & 0 & 0 \\ \mathbf{m}^m_{21} & \mathbf{0} & 0 & \mathbf{m}^m_{22} & \mathbf{0} & 0 & \mathbf{m}^m_{23} & \mathbf{0} & 0 & \mathbf{m}^m_{24} & \mathbf{0} & 0 \\ \mathbf{0} & \mathbf{m}^b_{21} & 0 & \mathbf{0} & \mathbf{m}^b_{23} & 0 & \mathbf{0} & \mathbf{m}^b_{23} & 0 & \mathbf{0} & \mathbf{m}^b_{24} & 0 \\ 0 & 0 & 0 & 0 & 0 & 0 & 0 & 0 & 0 & 0 & 0 & 0 \\ \mathbf{m}^m_{31} & \mathbf{0} & 0 & \mathbf{m}^m_{32} & \mathbf{0} & 0 & \mathbf{m}^m_{33} & \mathbf{0} & 0 & \mathbf{m}^m_{34} & \mathbf{0} & 0 \\ \mathbf{0} & \mathbf{m}^b_{31} & 0 & \mathbf{0} & \mathbf{m}^b_{33} & 0 & \mathbf{0} & \mathbf{m}^b_{33} & 0 & \mathbf{0} & \mathbf{m}^b_{34} & 0 \\ 0 & 0 & 0 & 0 & 0 & 0 & 0 & 0 & 0 & 0 & 0 & 0 \\ \mathbf{m}^m_{41} & \mathbf{0} & 0 & \mathbf{m}^m_{44} & \mathbf{0} & 0 & \mathbf{m}^m_{43} & \mathbf{0} & 0 & \mathbf{m}^m_{44} & \mathbf{0} & 0 \\ \mathbf{0} & \mathbf{m}^b_{41} & 0 & \mathbf{0} & \mathbf{m}^b_{43} & 0 & \mathbf{0} & \mathbf{m}^b_{43} & 0 & \mathbf{0} & \mathbf{m}^b_{44} & 0 \\ 0 & 0 & 0 & 0 & 0 & 0 & 0 & 0 & 0 & 0 & 0 & 0 \end{array}\right] \end{array} \begin{array}{l} \left.\begin{array}{c} \\ \\ \\ \end{array}\right\} \text{node 1} \\ \left.\begin{array}{c} \\ \\ \\ \end{array}\right\} \text{node 2} \\ \left.\begin{array}{c} \\ \\ \\ \end{array}\right\} \text{node 3} \\ \left.\begin{array}{c} \\ \\ \\ \end{array}\right\} \text{node 4} \end{array}$$

Stiffness matrix superposition

$$\mathbf{k} = \begin{array}{c} \begin{array}{cccc} \overbrace{\qquad\qquad\qquad}^{\text{node 1}} & \overbrace{\qquad\qquad\qquad}^{\text{node 2}} & \overbrace{\qquad\qquad\qquad}^{\text{node 3}} & \overbrace{\qquad\qquad\qquad}^{\text{node 4}} \end{array} \\ \left[\begin{array}{cccccccccccc} \mathbf{k}^m_{11} & \mathbf{0} & 0 & \mathbf{k}^m_{12} & \mathbf{0} & 0 & \mathbf{k}^m_{13} & \mathbf{0} & 0 & \mathbf{k}^m_{14} & \mathbf{0} & 0 \\ \mathbf{0} & \mathbf{k}^b_{11} & 0 & \mathbf{0} & \mathbf{k}^b_{12} & 0 & \mathbf{0} & \mathbf{k}^b_{13} & 0 & \mathbf{0} & \mathbf{k}^b_{14} & 0 \\ 0 & 0 & 0 & 0 & 0 & 0 & 0 & 0 & 0 & 0 & 0 & 0 \\ \mathbf{k}^m_{21} & \mathbf{0} & 0 & \mathbf{k}^m_{22} & \mathbf{0} & 0 & \mathbf{k}^m_{23} & \mathbf{0} & 0 & \mathbf{k}^m_{24} & \mathbf{0} & 0 \\ \mathbf{0} & \mathbf{k}^b_{21} & 0 & \mathbf{0} & \mathbf{k}^b_{23} & 0 & \mathbf{0} & \mathbf{k}^b_{23} & 0 & \mathbf{0} & \mathbf{k}^b_{24} & 0 \\ 0 & 0 & 0 & 0 & 0 & 0 & 0 & 0 & 0 & 0 & 0 & 0 \\ \mathbf{k}^m_{31} & \mathbf{0} & 0 & \mathbf{k}^m_{32} & \mathbf{0} & 0 & \mathbf{k}^m_{33} & \mathbf{0} & 0 & \mathbf{k}^m_{34} & \mathbf{0} & 0 \\ \mathbf{0} & \mathbf{k}^b_{31} & 0 & \mathbf{0} & \mathbf{k}^b_{33} & 0 & \mathbf{0} & \mathbf{k}^b_{33} & 0 & \mathbf{0} & \mathbf{k}^b_{34} & 0 \\ 0 & 0 & 0 & 0 & 0 & 0 & 0 & 0 & 0 & 0 & 0 & 0 \\ \mathbf{k}^m_{41} & \mathbf{0} & 0 & \mathbf{k}^m_{44} & \mathbf{0} & 0 & \mathbf{k}^m_{43} & \mathbf{0} & 0 & \mathbf{k}^m_{44} & \mathbf{0} & 0 \\ \mathbf{0} & \mathbf{k}^b_{41} & 0 & \mathbf{0} & \mathbf{k}^b_{43} & 0 & \mathbf{0} & \mathbf{k}^b_{43} & 0 & \mathbf{0} & \mathbf{k}^b_{44} & 0 \\ 0 & 0 & 0 & 0 & 0 & 0 & 0 & 0 & 0 & 0 & 0 & 0 \end{array}\right] \end{array} \begin{array}{l} \left.\begin{array}{c} \\ \\ \\ \end{array}\right\} \text{node 1} \\ \left.\begin{array}{c} \\ \\ \\ \end{array}\right\} \text{node 2} \\ \left.\begin{array}{c} \\ \\ \\ \end{array}\right\} \text{node 3} \\ \left.\begin{array}{c} \\ \\ \\ \end{array}\right\} \text{node 4} \end{array}$$

Abaqus modeling

Type	Poisson’s ration	Young’s modulus	density	length	width	thickness
Steel	0.3	200e9	7700 kg/m3	0.3 m	0.3 m	0.006 m

4 elements – 9 nodes

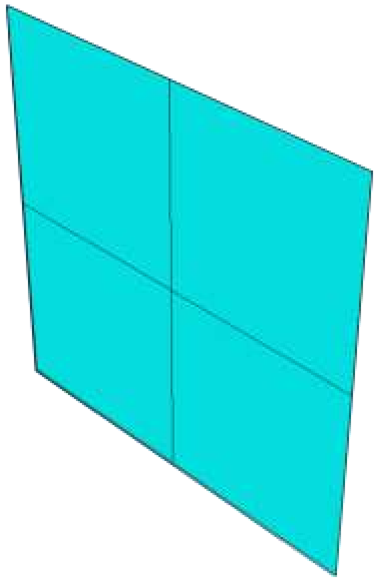

900 elements – 961 nodes

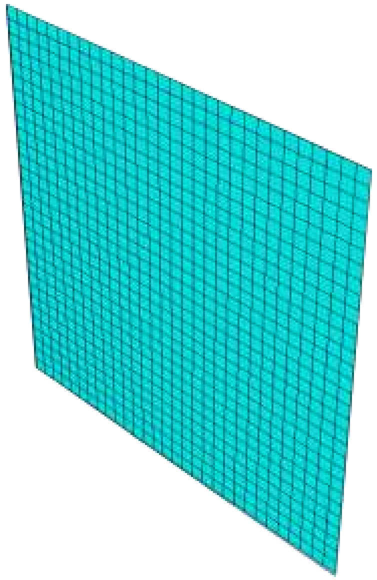

The plate was modeled in a free-free mode

Abaqus modeling (4 elements)

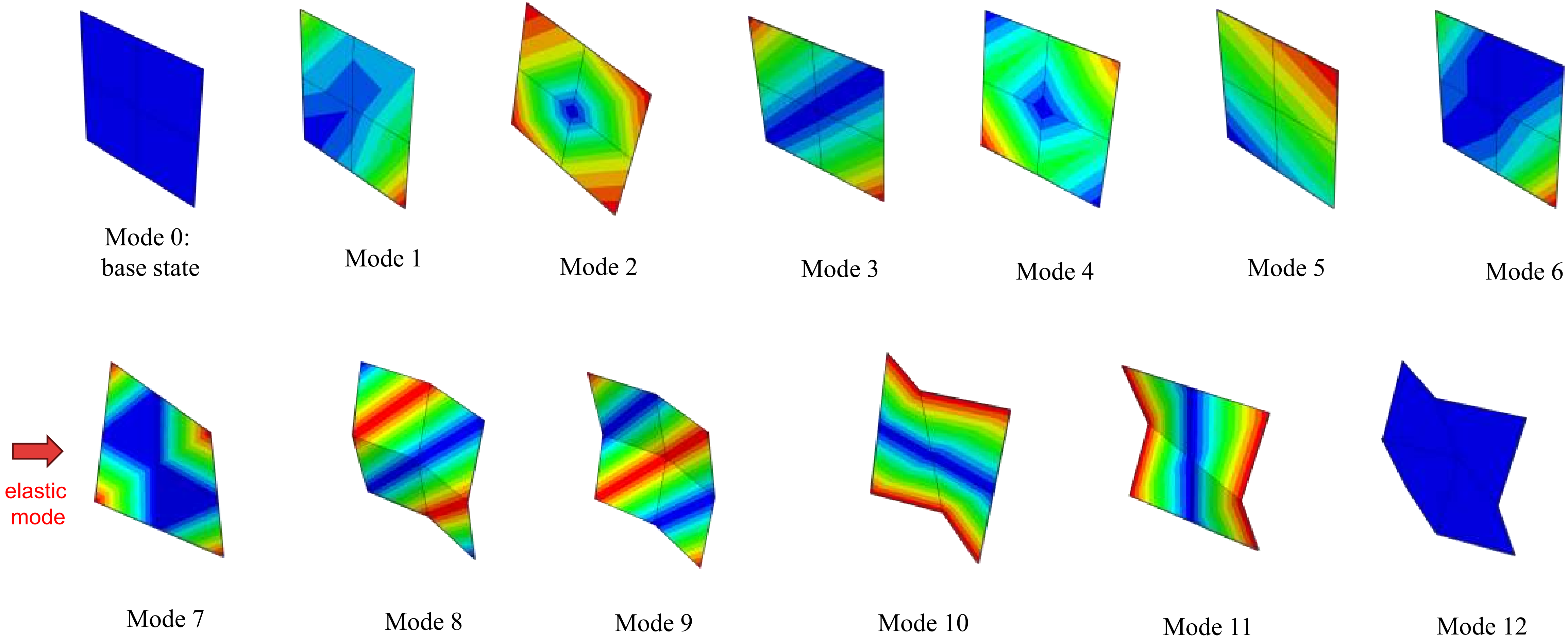

Abaqus modeling (900 elements)

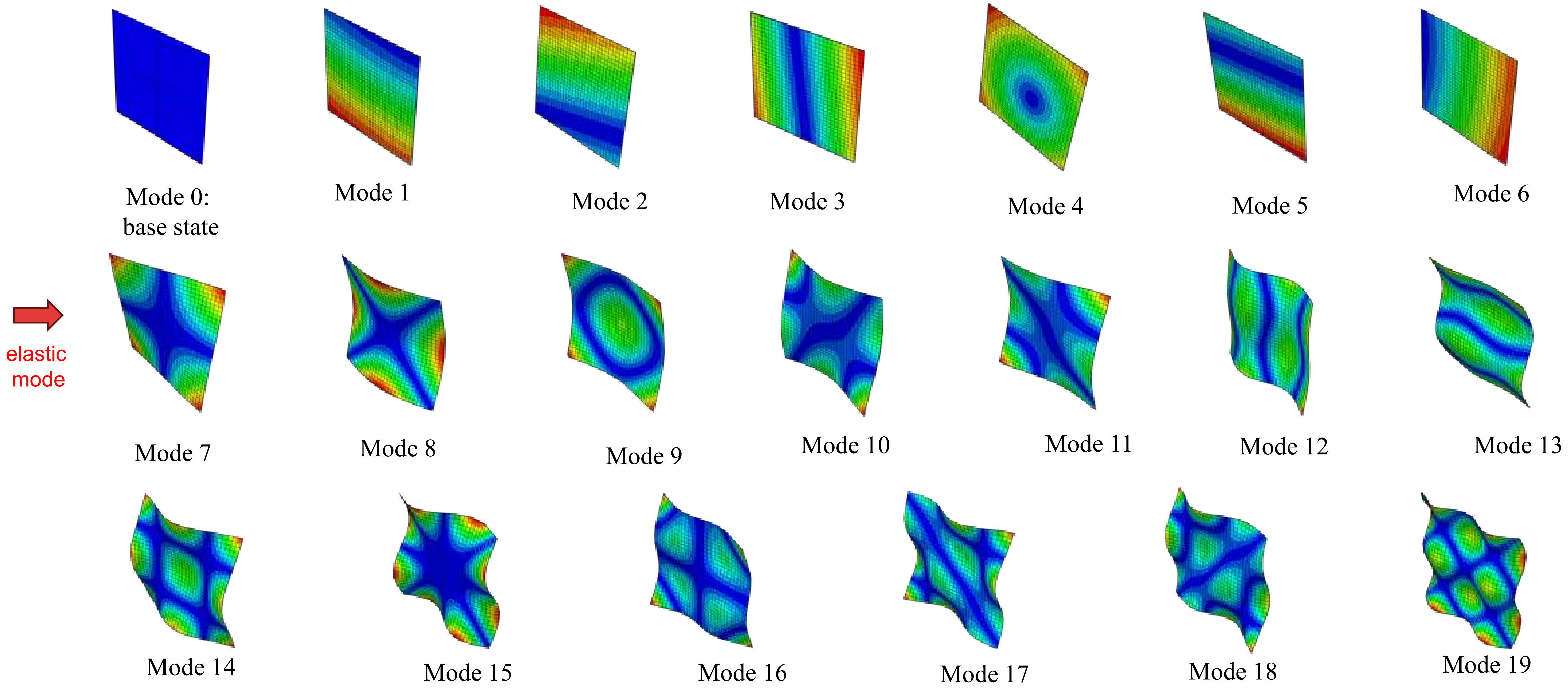

Mode Frequency

Step/Frame

Step Name	Description
Step-1	

4 elements

Frame

Index	Description
0	Increment 0: Base State
1	Mode 1: Value = -3.19909E-07 Freq = 0.0000 (cycles/time)
2	Mode 2: Value = -2.69152E-07 Freq = 0.0000 (cycles/time)
3	Mode 3: Value = -1.24332E-07 Freq = 0.0000 (cycles/time)
4	Mode 4: Value = -8.33534E-08 Freq = 0.0000 (cycles/time)
5	Mode 5: Value = -4.33065E-08 Freq = 0.0000 (cycles/time)
6	Mode 6: Value = -3.72529E-09 Freq = 0.0000 (cycles/time)
7	Mode 7: Value = 2.12713E+06 Freq = 232.12 (cycles/time)
8	Mode 8: Value = 5.66377E+06 Freq = 378.77 (cycles/time)
9	Mode 9: Value = 1.05068E+07 Freq = 515.89 (cycles/time)
10	Mode 10: Value = 1.41477E+07 Freq = 598.64 (cycles/time)
11	Mode 11: Value = 1.41477E+07 Freq = 598.64 (cycles/time)
12	Mode 12: Value = 3.52346E+07 Freq = 944.72 (cycles/time)

Step/Frame

Step Name	Description
Step-1	

900 elements

Frame

Index	Description
0	Increment 0: Base State
1	Mode 1: Value = 2.11708E-06 Freq = 2.31573E-04 (cycles/time)
2	Mode 2: Value = 3.40977E-06 Freq = 2.93888E-04 (cycles/time)
3	Mode 3: Value = 5.05996E-06 Freq = 3.58009E-04 (cycles/time)
4	Mode 4: Value = 6.18608E-06 Freq = 3.95847E-04 (cycles/time)
5	Mode 5: Value = 7.60294E-06 Freq = 4.38845E-04 (cycles/time)
6	Mode 6: Value = 1.44800E-05 Freq = 6.05625E-04 (cycles/time)
7	Mode 7: Value = 1.89263E+06 Freq = 218.95 (cycles/time)
8	Mode 8: Value = 4.05830E+06 Freq = 320.62 (cycles/time)
9	Mode 9: Value = 6.23002E+06 Freq = 397.25 (cycles/time)
10	Mode 10: Value = 1.26330E+07 Freq = 565.68 (cycles/time)
11	Mode 11: Value = 1.26330E+07 Freq = 565.68 (cycles/time)
12	Mode 12: Value = 3.95886E+07 Freq = 1001.4 (cycles/time)
13	Mode 13: Value = 3.95886E+07 Freq = 1001.4 (cycles/time)
14	Mode 14: Value = 4.20637E+07 Freq = 1032.2 (cycles/time)
15	Mode 15: Value = 5.01417E+07 Freq = 1127.0 (cycles/time)
16	Mode 16: Value = 6.26389E+07 Freq = 1259.6 (cycles/time)
17	Mode 17: Value = 1.15204E+08 Freq = 1708.3 (cycles/time)
18	Mode 18: Value = 1.15204E+08 Freq = 1708.3 (cycles/time)
19	Mode 19: Value = 1.46137E+08 Freq = 1924.0 (cycles/time)

Base state estimation with GE

INITIAL STATE

Mode	Abaqus (4 element, 9_nodes)	Generalized Eigenvalue	Error (abs)
7	232.12	232.027	0.0093
8	378.77	379.044	0.274
9	515.89	515.983	0.0093
10	598.64	598.768	0.128
11	598.64	598.768	0.128
12	944.72	945.03	0.31

Single state change with GE and LEMP

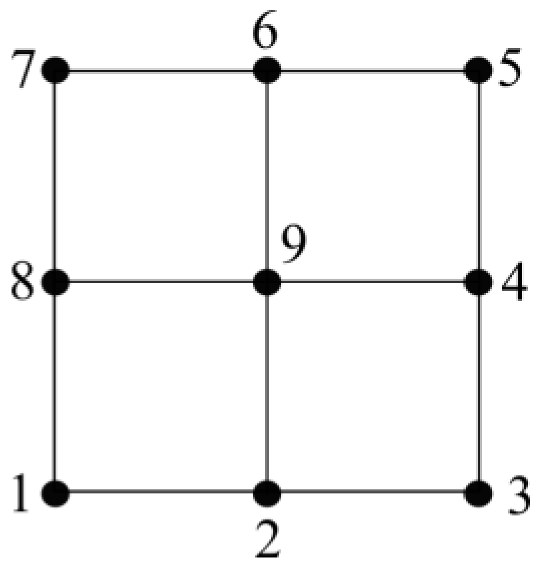

decreasing Stiffness value by 5e100 N/m at deflection (w) DOF of z-axis

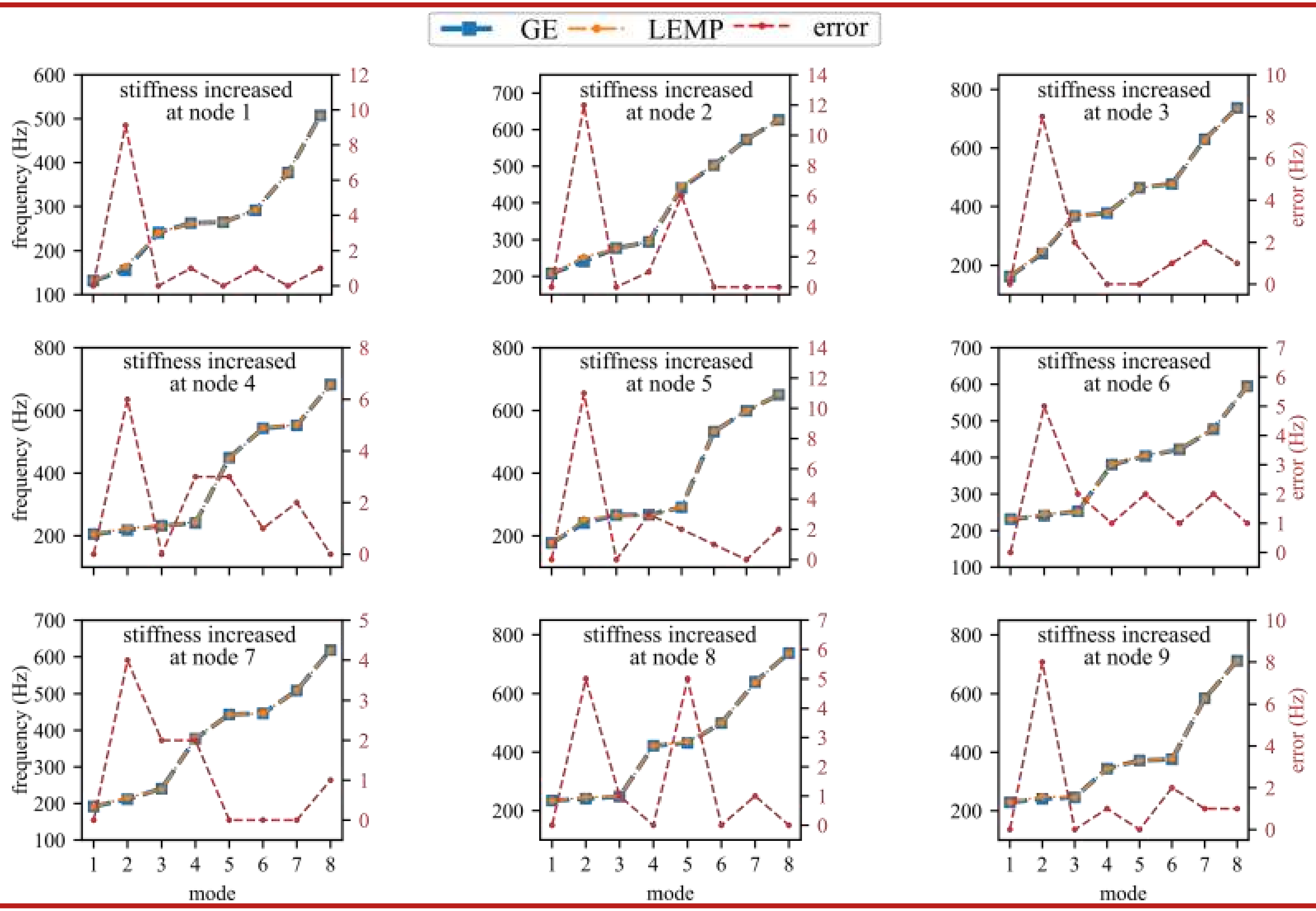

Single state change with GE and LEMP

Model update accuracy and timing

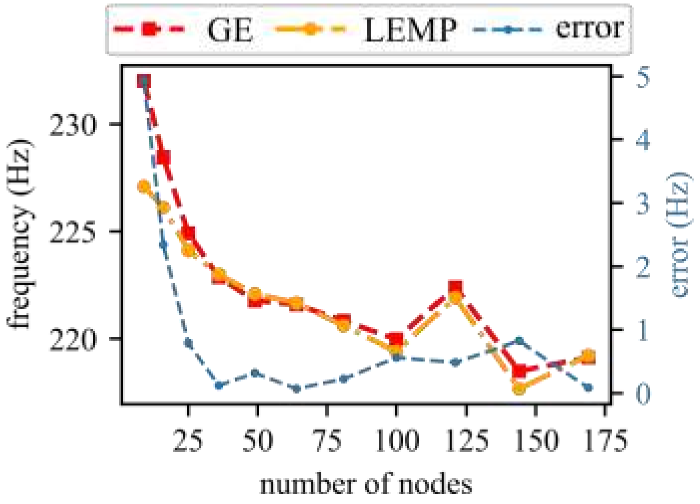

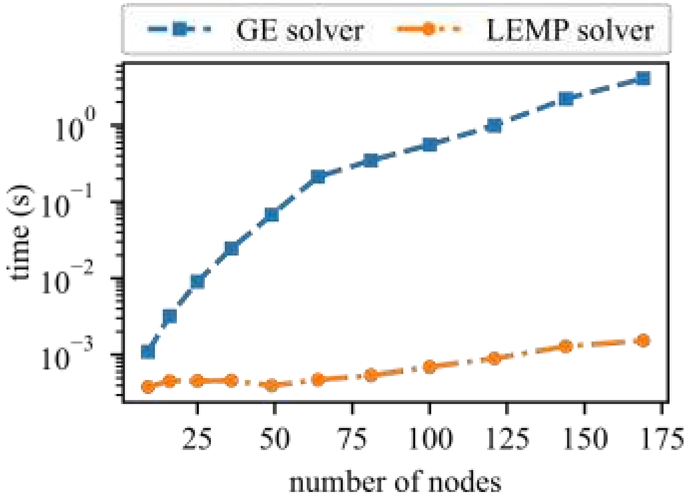

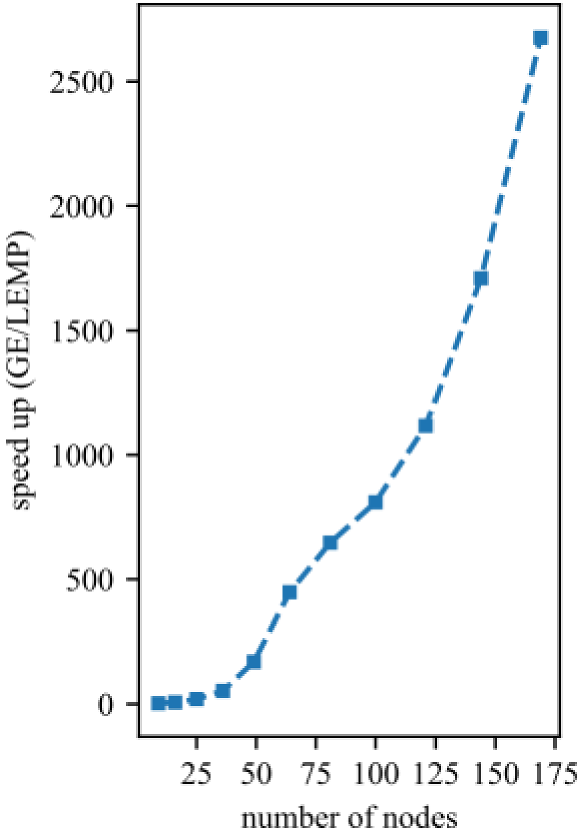

Only the first elastic mode was used for the frequency plot

PCB schematic

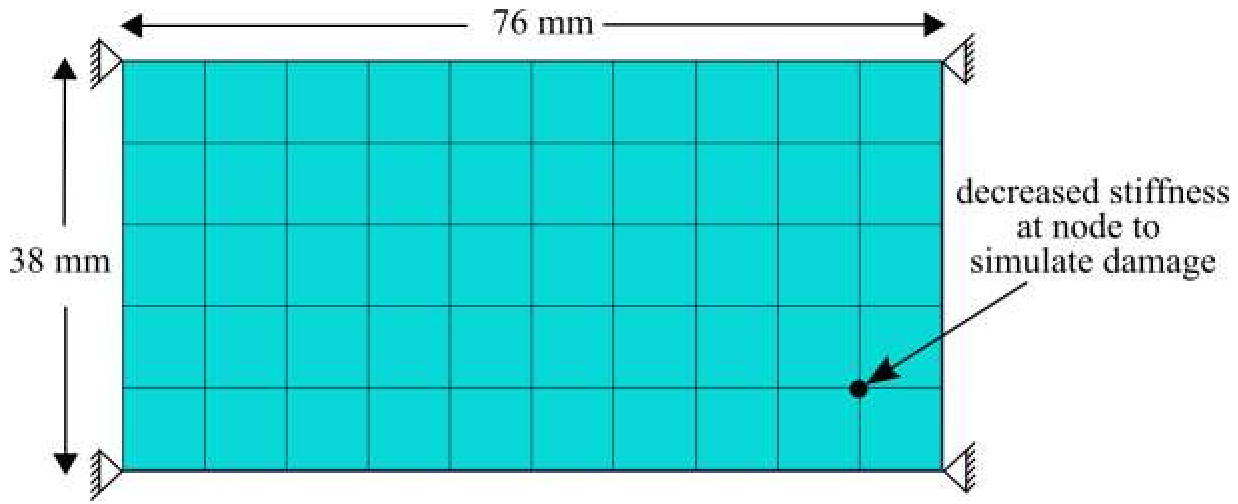

Single state change with GE and LEMP

INITIAL STATE

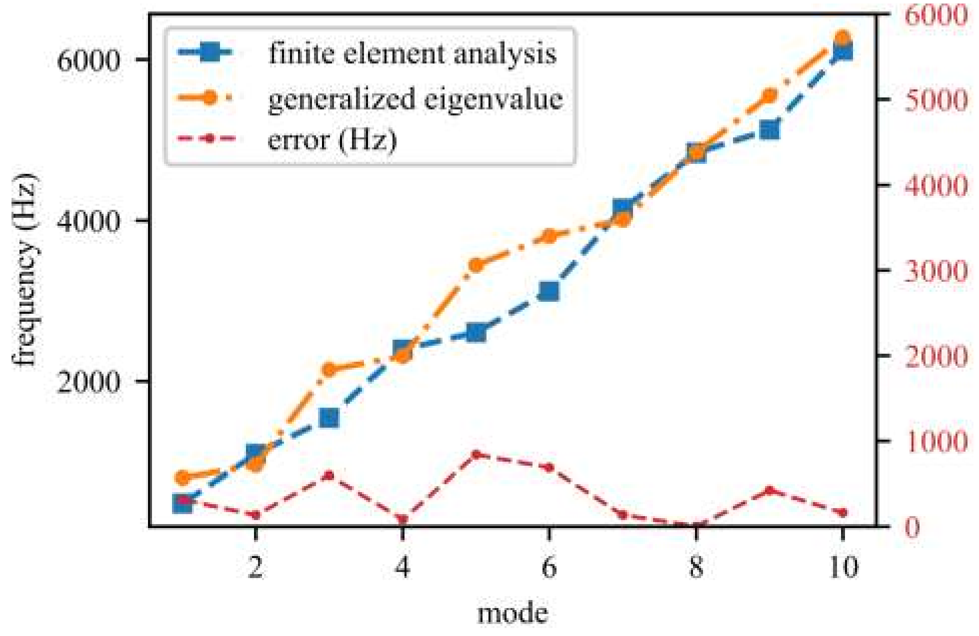

FINAL STATE

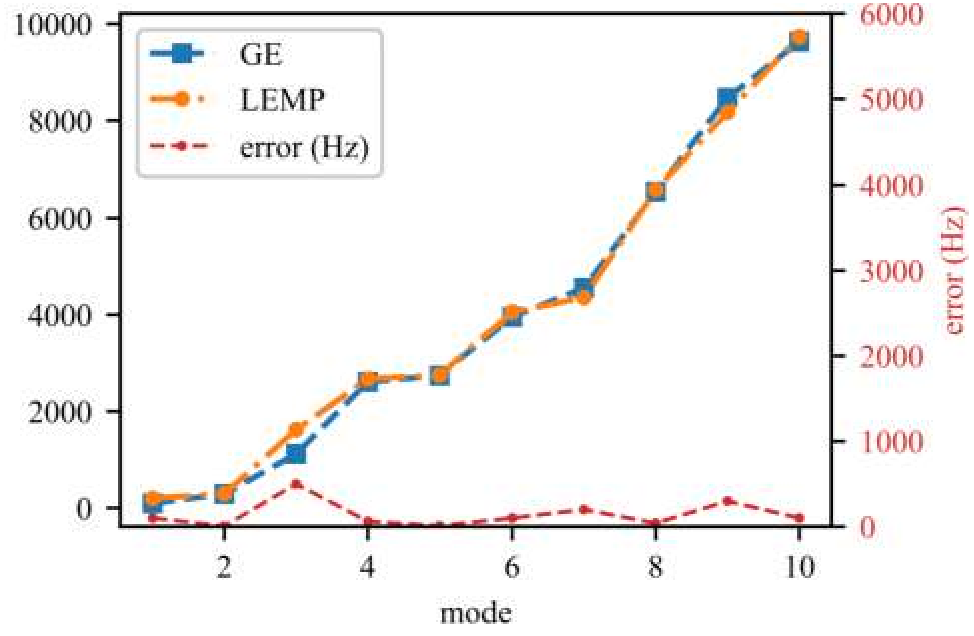

Upcoming works

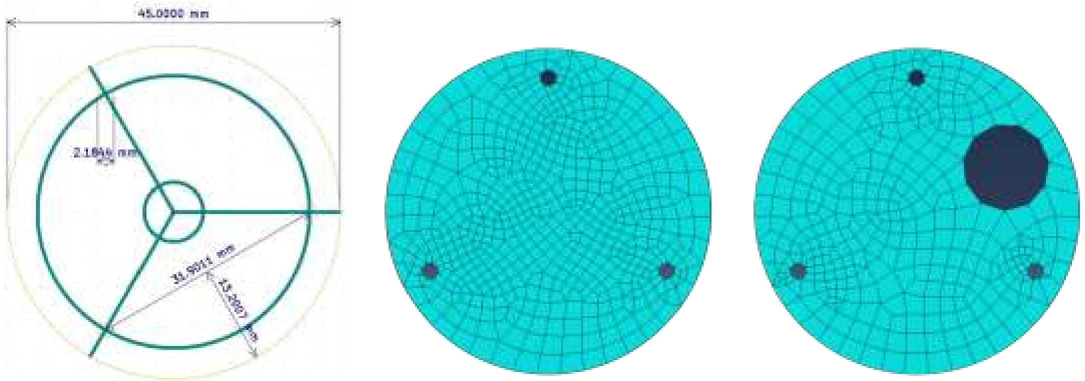

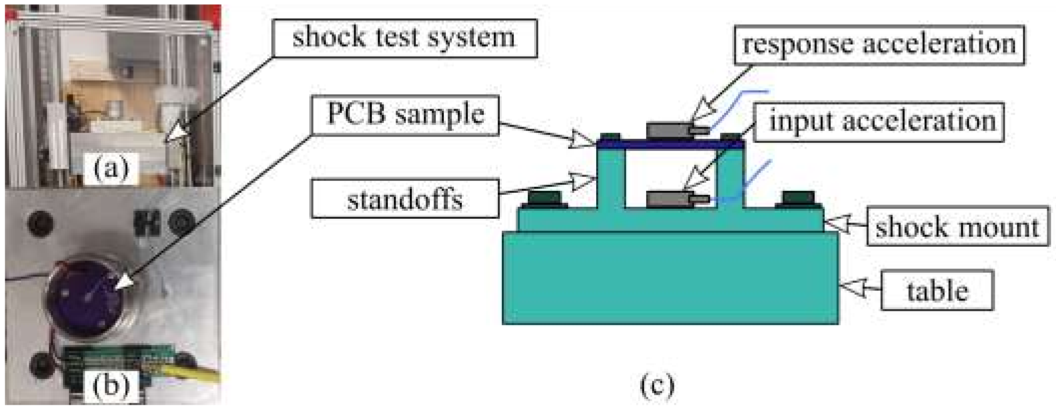

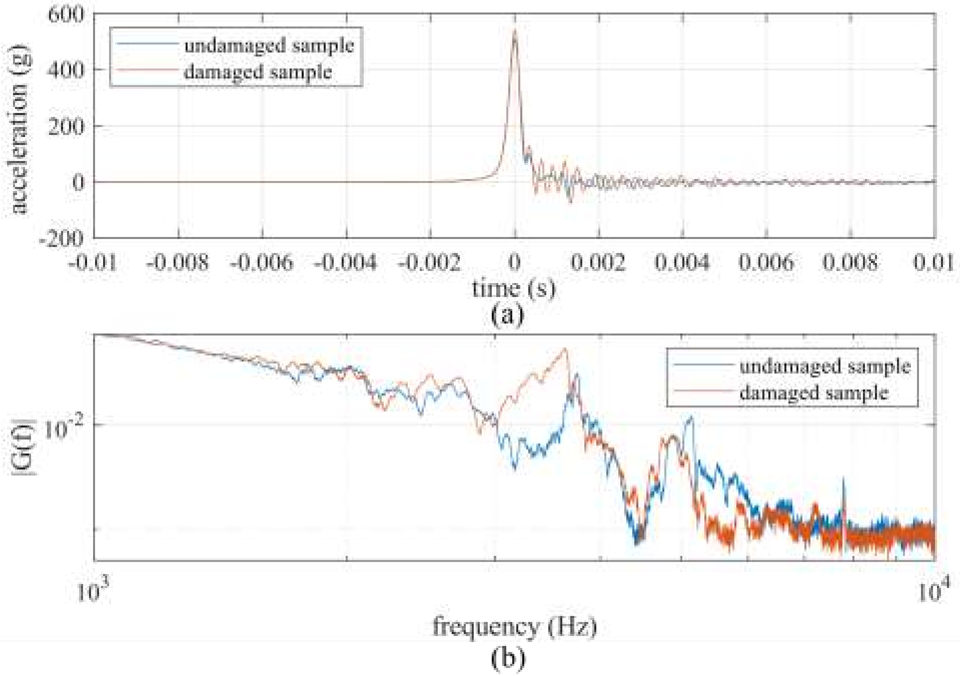

Next Generation Electronic Packaging

Thorough collaborations with the AFRL we are working on enabling technology for

- Fuzes with real-time decision-making capabilities
- Fuzes that can “adapt” to their condition
- Fuzes that are resilient to impact (e.g. after an impact, the are just as strong as before)
- Funded through an AFOSR YIP

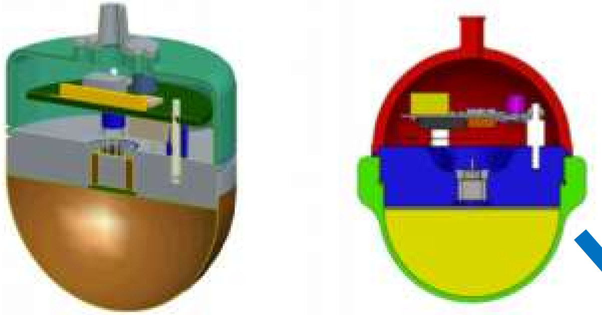

Embedded fuze design are being designed for enhanced safety and reduced cost.

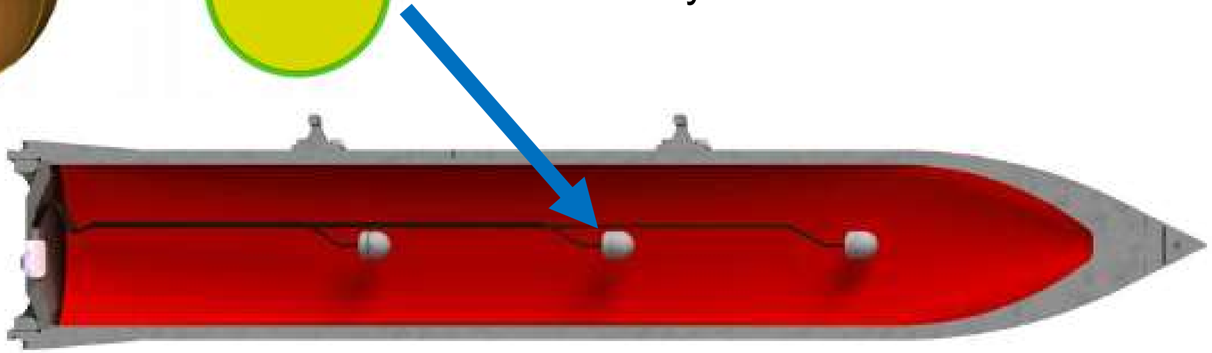

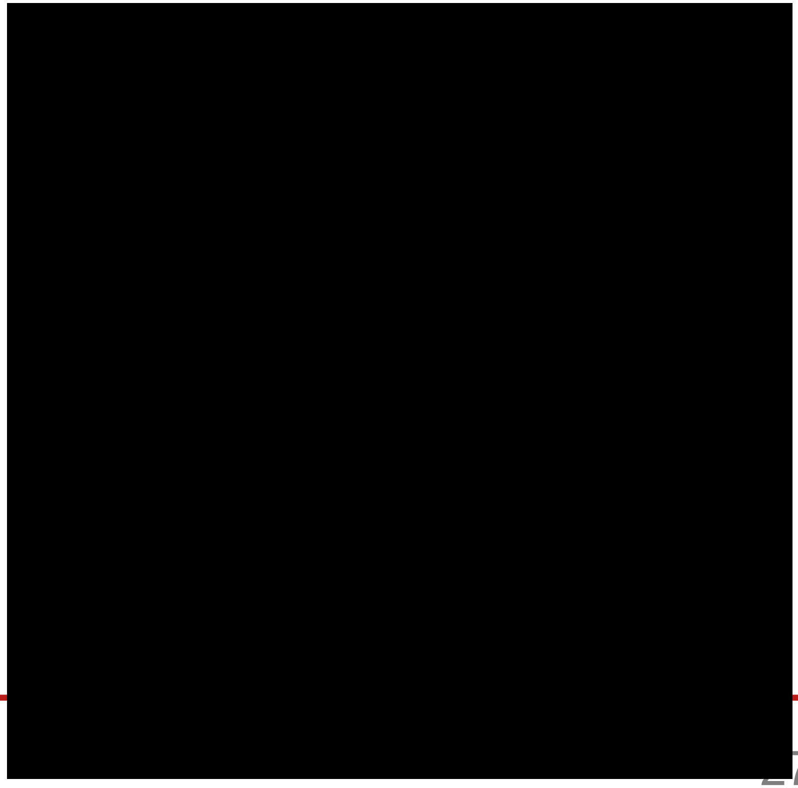

SAND2019-5293C

Conclusion

- The LEMP algorithm can be useful for faster solving of system equation for 2D structures because of large matrix size.

- LEMP accuracy compared to the Generalized Eigenvalue procedure is good.

Acknowledgement

This material is based upon work supported by the Air Force Office of Scientific Research (AFOSR) through award no. FA9550-21-1-0083. This work is also partly supported by the National Science Foundation Grant numbers 1850012 and 1956071. The support of these agencies is gratefully acknowledged. Any opinions, findings, conclusions, or recommendations expressed in this material are those of the authors, and they do not necessarily reflect the views of the National Science Foundation or the United States Air Force.

THANKS!

Name: Emmanuel Ogunniyi

Title: Graduate Research Assistant

Email: ogunniyi@email.sc.edu

Social

UofSC South Carolina